Table 3. Baseline Characteristics of Patients

	Surgical Group (n=42)	Nonsurgical Group (n=38)	*P* Value
Mean age±SD, y	42.5±11.3	41.4±12.2	0.34
Female ratio	66.7%	73.7%	0.49
Hypertension (%)	7 (16.7)	9 (23.7)	0.43
Diabetes mellitus (%)	1 (2.4)	2 (5.3)	0.46
Hyperlipidemia (%)	2 (4.8)	2 (5.3)	0.65
Valvular heart disease (%)	0 (0.0)	0 (0.0)	
Atrial fibrillation (%)	0 (0.0)	0 (0.0)	
Moyamoya disease in relatives (%)	6 (14.3)	1 (2.6)	0.07
History of hemorrhagic stroke (%)	4 (9.5)	4 (10.5)	0.59
History of ischemic events (%)	12 (28.6)	10 (26.3)	0.82
Hemorrhagic types			
Intraparenchymal (ICH)	14	8	0.22
Extraparenchymal extension			
ICH+IVH	26	29	
SAH only	2	1	
Site of hemorrhage			
Anterior (type A)*	24	21	0.87
Posterior (type B)†	18	17	

ICH indicates intracerebral hemorrhage; IVH, intraventricular hemorrhage; and SAH, subarachnoid hemorrhage.

*Hemorrhage attributed to rupture of the anterior collateral vessels (eg, caudate nucleus or putamen).

†Hemorrhage attributed to rupture of the posterior collateral vessels (eg, thalamus or trigone of the lateral ventricle).

In the surgical group, all patients but 1 underwent bilateral direct anastomotic bypass. One patient received direct bypass on one side and indirect bypass on the other side because no cortical artery feasible for direct anastomosis could be identified in the operative field. In the nonsurgical group, all patients were treated conservatively with no protocol violation. All patients but 1 were observed until the occurrence of adverse events compatible with end points or until 5 years had elapsed after enrollment. The murder of 1 patient in the surgical group at the point of 1.95 years after enrollment ended that patient's follow-up. The event-free period of this case was included in the statistical analysis. However, this event was dealt with as a dropout and not as an end point because it had no relation to the patient's medical issues. The mean follow-up period was 4.32 years (4.46 years in the surgical group and 4.17 in the nonsurgical group).

Study Outcomes

The last patient completed the 5-year follow-up in June 2013. Table 4 shows the outcomes of the patients. The primary end point was observed in 6 (14.3%) in the surgical group and 13 (34.2%) in the nonsurgical group. In the surgical group, 5 patients experienced rebleeding attacks and 1 patient had a completed ischemic stroke during the follow-up period. In the nonsurgical group, 12 patients experienced rebleeding attacks and 1 patient had crescendo TIAs requiring emergent bypass surgery as determined by the attendant neurologist. Accordingly, the secondary end point was observed in 5 (11.9%) in the surgical group and 12 (31.6%) in the nonsurgical group. Cox regression analysis revealed that the hazard ratios of the surgical group compared with the nonsurgical group were 0.391 (95% confidence interval, 0.148–1.029) as to the primary end point and 0.355 (95% confidence interval, 0.125–1.009) as to the secondary end point. Figure 2 shows the Kaplan–Meier cumulative curves for the analysis of the primary and secondary end points. The log-rank test revealed that the surgical group was at significantly lower risk than the nonsurgical group for both the primary end point (3.2%/y versus 8.2%/y; P=0.048) and the secondary end point (2.7%/y versus 7.6%/y; P=0.042).

Perioperative Complications

Among the 84 surgical procedures for the 42 patients in the surgical group, perioperative complications were observed in 8 cases (9.5%). Symptoms of local hyperperfusion around the anastomotic sites were the most frequent (3 cases). Other perioperative events consisted of TIA, seizure, local vasogenic edema, scalp bedsore, and tear of a subcutaneous drainage tube. Seven of the 8 events were clinically transient, and no sequelae remained. One patient with local hyperperfusion syndrome showed a deterioration in modified Rankin disability scale score. This event, however, was not severe enough to fulfill the criteria of the end point.

Discussion

It is known that about one half of the adult patients with moyamoya disease have intracranial hemorrhage, whereas most pediatric cases present with cerebral ischemia.[1–3] Typically, the hemorrhage involves the thalamus and basal ganglia with

Table 4. Details of Outcomes and Cox Regression Analysis

	Surgical Group (n=42)		Nonsurgical Group (n=38)			
	n	Rate, %	n	Rate, %	Hazard Ratio (95% CI)	*P* Value
Primary end point	6	14.3	13	34.2	0.391 (0.148–1.029)	0.057
Recurrent bleeding	5	11.9	12	31.6	0.355 (0.125–1.009)	0.052
Completed stroke	1	2.4	0	0.0	…	…
Crescendo TIA (bypass required)	0	0.0	1	2.6	…	…
Secondary end point (recurrent bleeding or related death/severe disability)	5	11.9	12	31.6	0.355 (0.125–1.009)	0.052

CI indicates confidence interval; and TIA transient ischemic attack.

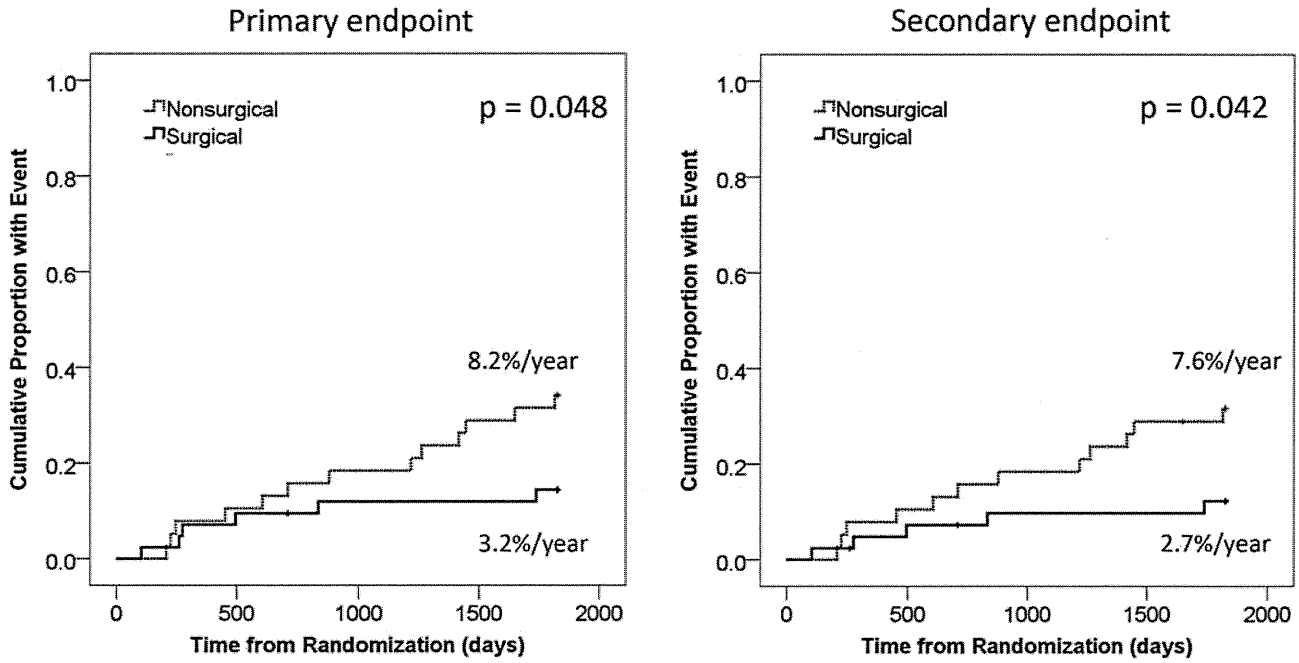

Figure 2. Kaplan–Meier cumulative curves for end points.

frequent perforation to the ventricles. It is speculated that long-term hemodynamic overstress can induce pathological change in the dilated collateral vessels such as lenticulostriate arteries, choroidal arteries, and other basal moyamoya vessels, which leads to the bleeding.[1,2] The rupture of microaneurysms formed in the collateral vessels has also been recognized.[7] Such bleeding attacks, which are potentially fatal, seriously affect the patient's prognosis.[8]

The natural history of hemorrhagic moyamoya disease is extremely poor because of the high rate of recurrent bleeding attacks. Kobayashi et al[9] reported that 33.3% of the patients who were conservatively treated had rebleeding attacks during the follow-up period of mean 6.7 years and estimated the annual rebleeding rate to be 7.09%/y. Because the majority of the patients were in their 30s to 50s at the onset of hemorrhage,[3,10] this annual rate indicates that, over a long period, rebleeding attacks seriously threaten their lives. No therapeutic method for preventing rebleeding attacks, however, has been established. No evidence exists that treatment of hypertension reduces the rebleeding rate. Even the relationship between hypertension and intracranial hemorrhage in moyamoya disease has not been proven.

At present, the only promising strategy is extracranial–intracranial bypass. In ischemic moyamoya disease, angiography often demonstrates that moyamoya vessels can diminish after bypass surgery.[4] It is likely that the dominant bypass flow reduces the burden on moyamoya vessels to maintain the cerebral blood flow, which results in relief of hemodynamic stress. Microaneurysms in collateral vessels that disappear after surgery have also been reported.[11,12] Consequently, a hypothesis has emerged that bypass surgery can also reduce the long-term hemodynamic stress in hemorrhagic moyamoya disease and prevent rebleeding attacks. In fact, some authors have reported the effectiveness of bypass for hemorrhagic moyamoya disease. Kawaguchi et al[13] revealed that superficial temporal artery–middle cerebral artery bypass reduced the rate of hemorrhagic and ischemic stroke. Karasawa et al[14] reported that patients who had undergone bypass surgery experienced rebleeding attacks less frequently than those treated conservatively. Several authors, on the contrary, failed to reveal the effectiveness of bypass.[8,15] A multicenter retrospective questionnaire study conducted by Fujii et al[15] revealed that rebleeding attacks were less frequent in patients who had undergone bypass surgery than in the nonsurgical cases, but the difference was not statistically significant. All previous reports, however, were retrospective studies that potentially contain various biases. Consequently, the effectiveness of bypass surgery on hemorrhagic moyamoya disease has remained unclear.

The JAM Trial, which is the first prospective, randomized, controlled trial focused on moyamoya disease, has demonstrated how bypass surgery affects patients' prognosis and the rebleeding rate in hemorrhagic moyamoya disease. Kaplan–Meier survival analysis revealed that direct bypass surgery significantly decreased the rate of both all adverse events (primary end point) and rebleeding attacks (secondary end point) during the following 5 years. These results strongly suggest that the newly established bypass flow can influence the hemodynamic state of the collateral vessels and lessen their overstress. This study required direct anastomotic bypass because indirect bypass alone can fail to establish sufficient extracranial–intracranial collateral flow in adult patients.[3,4] To ensure the quality of the trial, every institute was requested to report all patients who were assessed for eligibility but were not enrolled in the study, and bypass surgery for these cases was prohibited. In addition, no protocol violation was observed regarding the enrolled patients.

Care must be taken when interpreting the results of the JAM Trial. First, the result was statistically marginal. Kaplan–Meier survival analysis revealed the significant benefits of bypass surgery, but the *P* values of the primary and secondary

end points were 0.048 and 0.042, respectively, which are close to 0.05. In the Cox regression analysis, the upper limit of the 95% confidence interval of the hazard ratio was 1.029 for the primary end point and 1.009 for the secondary end point, both of which slightly exceed 1.0. Therefore, the authors cannot declare with assurance that bypass surgery is absolutely superior to conservative therapy. This difference can be attributed to the small sample size. As mentioned earlier, the optimal sample size initially calculated was larger. Hemorrhagic moyamoya disease, however, is not common, and recruitment of patients with good modified Rankin disability scale scores was far more difficult than expected. Considering that an excessively long registration period would degrade the quality of this trial, the number of the cases was reduced.

Second, some limitations apply to the JAM Trial regarding generalization. All institutes participating in the trial had sufficient experience with direct bypass surgery for moyamoya disease, and only registered surgeons were allowed to operate on patients. Consequently, the rate of perioperative complications, including transient events, turned out to be 9.5%, and permanent severe disability was not observed. The authors think that ensuring the quality of surgeons is indispensable to this kind of randomized trial involving surgery. As for interpretation of the results, however, it should be emphasized that the results do not necessarily apply to all neurosurgical institutes.

Third, and perhaps most important, the JAM Trial has only revealed the effect of bypass surgery within 5 years and does not suggest an improved prognosis for the surgical group thereafter. It is well known that recurrent bleeding can take place >10 years after the initial attack.[9] Therefore, patients enrolled in the JAM Trial should be observed for longer periods in the future. The JAM Trial Executive and Steering Committee has already decided to continue with patient follow-up and report the 10-year results. Subanalyses regarding the site of initial and recurrent hemorrhage, hemodynamic impairment evaluated by single-photon emission computed tomography, and angiographic reduction of moyamoya vessels after bypass surgery should also be performed, and the results should be reported.

Conclusions

Although statistically marginal, the JAM Trial revealed that direct bypass surgery for adult patients with hemorrhagic moyamoya disease reduces the rebleeding rate and improves a patient's prognosis during the 5 years after enrollment. To determine the long-term benefits of surgery, further follow-up is required.

Appendix: Study Organization

The Research Committee on Moyamoya Disease of the Japanese Ministry of Health, Labour and Welfare

Principal Investigator and Chair

1999 to 2005: Takashi Yoshimoto, MD, PhD
2005 to 2013: Nobuo Hashimoto, MD, PhDJAM Trial Group

Central Office and Data Management Center

Department of Neurosurgery, Graduate School of Medicine, Kyoto University, Kyoto, Japan: Susumu Miyamoto, MD, PhD; Keisuke Yamada, MD, PhD; and Jun C. Takahashi, MD, PhD.

Statistical Center

Department of Public Health, Tohoku University Graduate School of Medicine, Sendai, Japan: Ichiro Tsuji, MD, PhD; and Yasutake Tomata PhD.

Randomization and Quality Control Center

Department of General Internal Medicine, St. Luke's International Hospital, Tokyo, Japan: Tsuguya Fukui, MD, PhD.

Executive and Steering Committee

Takashi Yoshimoto, MD, PhD (principal investigator); Susumu Miyamoto, MD, PhD (project director; neurosurgery); Yasushi Okada, MD, PhD (co-project director; neurology), Tsuguya Fukui, MD, PhD; Ichiro Tsuji, MD, PhD; Yasuo Fukuuchi, MD, PhD; Takashi Ohmoto, MD, PhD; Yasuo Kuwabara, MD, PhD; Jyoji Nakagawara, MD; and Izumi Nagata MD, PhD.

Participating Centers and Researchers

Chiba University Graduate School of Medicine, Chiba, Japan: Junichi Ono, Toshio Machida, and Ryuji Sakakibara.

Chugoku Rousai Hospital, Kure, Japan: Kanji Yamane and Shinji Okita.

Gifu University Graduate School of Medicine, Gifu, Japan: Toru Iwama and Yasuhiko Kaku.

Gunma University, Maebashi, Japan: Nobuhito Saito.

Graduate School of Medicine, Kyoto University, Kyoto, Japan: Susumu Miyamoto, Keisuke Yamada, Hidenao Fukuyama, and Jun C. Takahashi.

Graduate School of Medicine Hokkaido University, Sapporo, Japan: Kiyohiro Houkin, Satoshi Kuroda, Ichiro Yabe, and Fumio Moriwaka.

Iwate Medical University, Morioka, Japan: Akira Ogawa, Kuniaki Ogasawara, and Kenji Yoshida.

Kitasato University School of Medicine, Sagamihara, Japan: Kiyotaka Fujii, Masaru Yamada, Kimitoshi Sato, and Tsugio Akutsu.

Kurashiki Central Hospital, Kurashiki, Japan: Sen Yamagata.

Nagaoka Chuo General Hospital, Nagaoka, Japan: Shigekazu Takeuchi.

Nagasaki University Medical School, Nagasaki, Japan: Izumi Nagata, Kentaro Hayashi, and Nobutaka Horie.

Nagoya City University Medical School, Nagoya, Japan: Kazuo Yamada.

Nakamura Memorial Hospital, Sapporo, Japan: Jyoji Nakagawara, Toshiaki Osato, Toshiichi Watanabe, Kaori Honjo, and Kazuya Sako.

Nara Medical University, Kashihara, Japan: Hiroyuki Nakase, Shoichiro Kawaguchi, Fumihiko Nisimura, and Junichi Yamao.

National Cardiovascular Center, Suita, Japan: Susumu Miyamoto, Jun C. Takahashi, Hiroaki Naritomi, and Jyoji Nakagawara.

National Kyushu Medical Center, Fukuoka, Japan: Tooru Inoue, Yasushi Okada, and Hiroshi Abe (Fukuoka University).

Akita Research Institute for Brain and Blood Vessels, Akita, Japan: Akifumi Suzuki and Tatsuya Ishikawa.

Sapporo Medical University, Sapporo, Japan: Kiyohiro Houkin.

Tenri Hospital, Tenri, Japan: Yoshinori Akiyama and Toshihiko Suenaga.

Tohoku University Graduate School of Medicine, Sendai, Japan: Teiji Tominaga and Miki Fujimura.

Tokushima University, Tokushima, Japan: Shinji Nagahiro, Masaaki Uno, Kyoko Nishi, and Junichiro Satomi.

Tokyo Women's Medical University, Tokyo, Japan: Yoshikazu Okada, Akiji Kawashima, Kohji Yamaguchi, and Yukiko Tsutsumi.

Sources of Funding

The JAM Trial has been funded since 1999 by a grant from the Japanese Ministry of Health, Labour and Welfare as a major project of the Research Committee on Spontaneous Occlusion of the Circle of Willis (moyamoya disease).

Disclosures

None.

References

1. Kuroda S, Houkin K. Moyamoya disease: current concepts and future perspectives. *Lancet Neurol*. 2008;7:1056–1066.
2. Takahashi JC, Miyamoto S. Moyamoya disease: recent progress and outlook. *Neurol Med Chir (Tokyo)*. 2010;50:824–832.
3. Research Committee on the Pathology and Treatment of Spontaneous Occlusion of the Circle of Willis; Health Labour Sciences Research Grant for Research on Measures for Infractable Diseases. Guidelines for diagnosis and treatment of moyamoya disease (spontaneous occlusion of the circle of Willis). *Neurol Med Chir (Tokyo)*. 2012;52:245–266.
4. Houkin K, Kamiyama H, Abe H, Takahashi A, Kuroda S. Surgical therapy for adult moyamoya disease. Can surgical revascularization prevent the recurrence of intracerebral hemorrhage? *Stroke*. 1996;27:1342–1346.
5. Miyamoto S; Japan Adult Moyamoya Trial Group. Study design for a prospective randomized trial of extracranial-intracranial (EC-IC) bypass surgery for adults with moyamoya disease with hemorrhagic onset—the Japan Adult Moyamoya Trial Group. *Neurol Med Chir (Tokyo)*. 2004;44:218–219.
6. van Swieten JC, Koudstaal PJ, Visser MC, Schouten HJ, van Gijn J. Interobserver agreement for the assessment of handicap in stroke patients. *Stroke*. 1988;19:604–607.
7. Kawaguchi S, Sakaki T, Morimoto T, Kakizaki T, Kamada K. Characteristics of intracranial aneurysms associated with moyamoya disease. A review of 111 cases. *Acta Neurochir (Wien)*. 1996;138:1287–1294.
8. Yoshida Y, Yoshimoto T, Shirane R, Sakurai Y. Clinical course, surgical management, and long-term outcome of moyamoya patients with rebleeding after an episode of intracerebral hemorrhage: an extensive follow-up study. *Stroke*. 1999;30:2272–2276.
9. Kobayashi E, Saeki N, Oishi H, Hirai S, Yamaura A. Long-term natural history of hemorrhagic moyamoya disease in 42 patients. *J Neurosurg*. 2000;93:976–980.
10. Baba T, Houkin K, Kuroda S. Novel epidemiological features of moyamoya disease. *J Neurol Neurosurg Psychiatry*. 2008;79:900–904.
11. Kuroda S, Houkin K, Kamiyama H, Abe H. Effects of surgical revascularization on peripheral artery aneurysms in moyamoya disease: report of three cases. *Neurosurgery*. 2001;49:463–467.
12. Ni W, Xu F, Xu B, Liao Y, Gu Y, Song D. Disappearance of aneurysms associated with moyamoya disease after STA-MCA anastomosis with encephaloduro myosynangiosis. *J Clin Neurosci*. 2012;19:485–487.
13. Kawaguchi S, Okuno S, Sakaki T. Effect of direct arterial bypass on the prevention of future stroke in patients with the hemorrhagic variety of moyamoya disease. *J Neurosurg*. 2000;93:397–401.
14. Karasawa J, Hosoi K, Morisako T. *Revascularization for Hemorrhagic Moyamoya Disease. Research Committee on Spontaneous Occlusion of the Circle of Willis (Moyamoya Disease) of Ministry of Health Labor and Welfare: Annual Report 2000 (in Japanese)*. Tokyo, Japan: Ministry of Health, Labor, and Welfare; 2001:55–58.
15. Fujii K, Ikezaki K, Irikura K, Miyasaka Y, Fukui M. The efficacy of bypass surgery for the patients with hemorrhagic moyamoya disease. *Clin Neurol Neurosurg*. 1997;99(suppl 2):S194–S195.

Chronic Ischemia Alters Brain Microstructural Integrity and Cognitive Performance in Adult Moyamoya Disease

Ken Kazumata, MD; Khin Khin Tha, MD; Hisashi Narita, MD; Ichiro Kusumi, MD; Hideo Shichinohe, MD; Masaki Ito, MD; Naoki Nakayama, MD; Kiyohiro Houkin, MD

Background and Purpose—The mechanisms underlying frontal lobe dysfunction in moyamoya disease (MMD) are unknown. We aimed to determine whether chronic ischemia induces subtle microstructural brain changes in adult MMD and evaluated the association of changes with neuropsychological performance.

Methods—MRI, including 3-dimensional T1-weighted imaging and diffusion tensor imaging, was performed in 23 adult patients with MMD and 23 age-matched controls and gray matter density and major diffusion tensor imaging indices were compared between them; any alterations in the patients were tested for associations with age, ischemic symptoms, hemodynamic compromise, and neuropsychological performance.

Results—Decrease in gray matter density, associated with hemodynamic compromise ($P<0.05$), was observed in the posterior cingulate cortex of patients with MMD. Widespread reduction in fractional anisotropy and increases in radial diffusivity and mean diffusivity in some areas were also observed in bilateral cerebral white matter. The fractional anisotropy ($r=0.54$; $P<0.0001$) and radial diffusivity ($r=-0.41$; $P<0.01$) of white matter significantly associated with gray matter density of the cingulate cortex. The mean fractional anisotropy of the white matter tracts of the lateral prefrontal, cingulate, and inferior parietal regions were significantly associated with processing speed, executive function/attention, and working memory.

Conclusions—In adult MMD, there were more white matter abnormalities than gray matter changes. Disruption of white matter may play a pivotal role in the development of cognitive dysfunction. **(*Stroke*. 2015;46:354-360. DOI: 10.1161/STROKEAHA.114.007407.)**

Key Words: diffusion ■ ischemia ■ magnetic resonance imaging ■ moyamoya disease ■ white matter disease

Moyamoya disease (MMD) is characterized by the presence of net-like collateral vessels at the brain base that are caused by progressive major cerebral artery occlusion.[1] Executive function/attention and working memory, primarily mediated by the lateral prefrontal region, are impaired, suggesting that lateral prefrontal ischemia is responsible for neurocognitive dysfunction.[2,3] A recent investigation revealed the association of neurocognitive dysfunction with reduced cerebral blood flow.[3] Nevertheless, not all patients with neurocognitive dysfunction had cerebral infarction on conventional MRI. Thus, ischemia-induced subtle microstructural alterations, which are beyond the detectability of conventional MRI, underlie neurocognitive dysfunction in MMD.

Subtle gray matter changes, not shown on conventional MRI, are successfully detected in many diseases, such as mild cognitive impairment and schizophrenia, through voxel-by-voxel comparison of gray matter density on 3-dimensional (3D) MRI.[4,5] Diffusion tensor imaging (DTI) is reportedly highly sensitive to microstructural alterations in diffusion characteristics of white matter.[6–9] To the best of our knowledge, no reports have evaluated gray matter changes in MMD using 3D MRI. There are only few reports on DTI assessments of MMD white matter integrity.[6–8] Nevertheless, these reports used a specified region-of-interest approach and evaluated only 2 major DTI indices, such as fractional anisotropy (FA) and mean diffusivity (MD). Voxel-based analysis of white matter can provide detailed topographical characteristics of white matter integrity, and tractography can show the integrity of the major white matter tracts that run in anatomic regions. Furthermore, additional information for characterizing chronic ischemia-induced white matter damage can be extracted by incorporating other major DTI indices, such as axial diffusivity (AD) and radial diffusivity (RD).

Here, we investigated the brain's microstructure across different regions in adult MMD by a voxel-based analysis of gray and white matter and tractography, and evaluated the relationship of these microstructural alterations with hemodynamic compromise and neurocognitive dysfunction.

Received September 10, 2014; final revision received November 5, 2014; accepted November 26, 2014.

From the Departments of Neurosurgery (K.K., H.S., M.I., N.N., K.H.), Radiobiology and Medical Engineering (K.K.T.), and Psychiatry (H.N., I.K.), Hokkaido University Graduate School of Medicine, Sapporo, Japan.

The online-only Data Supplement is available with this article at http://stroke.ahajournals.org/lookup/suppl/doi:10.1161/STROKEAHA.114.007407/-/DC1.

Correspondence to Ken Kazumata, MD, Department of Neurosurgery, Hokkaido University Graduate School of Medicine, N 15 W 7, Kita, Sapporo 060-8638, Japan. Email kazumata@med.hokudai.ac.jp

***Stroke* is available at http://stroke.ahajournals.org** **DOI: 10.1161/STROKEAHA.114.007407**

Materials and Methods

Participants

This prospective study was approved by the Research Ethics Committee of Hokkaido University Hospital. Written informed consent was obtained from all participants.

The inclusion criteria were clinical diagnosis of idiopathic MMD according to the consensus criteria and guideline for MMD proposed by the Research Committee on Spontaneous Occlusion of the Circle of Willis and age of >20.[10] The exclusion criteria were quasi-moyamoya syndrome with conditions such as Down syndrome and neurofibromatosis, cortical infarction or subcortical lesion of >8 mm in the largest dimension on conventional MRI, intracranial hemorrhage, revascularization surgery before the study, apparent neurological deficit because of stroke, and comorbid illnesses that could affect cognition. After exclusions, 23 patients (6 men, 17 women, 21–58 years; mean age, 40.9±9.5 years) were enrolled. The selection period was 25 months (from April 2012 to April 2014).

The inclusion criteria for controls were no clinical evidence of psychiatric or neurological disorders, normal intelligence quotient as assessed by the Japanese version of the Nelson Adult Reading Test,[11] no brain lesions on conventional MRI, and no medication that could affect cognitive function. The control group also comprised 23 subjects (10 men, 13 women; 25–56 years; mean age, 39.0±8.1 years). The mean estimated intelligence quotient was 108.3±6.6.

Hemodynamic Status Assessment

Cerebrovascular reactivity assessed by single positron emission computed tomography was used to determine the hemodynamic status in patients with MMD. A cerebrovascular reactivity of <15% in the left- or right-middle cerebral artery territory was considered as a hemodynamic compromise. Single positron emission computed tomography was performed within 7 days from MRI in 18 patients (Appendix I in the online-only Data Supplement).

Neuropsychological Assessment

The neuropsychological assessment was performed in all patients with MMD. A neuropsychological battery sensitive to cognitive dysfunction because of frontal lobe injury was used and comprised the Wechsler Adult Intelligent scale-III, Wisconsin Card Sorting test, Trail Making Test (TMT; parts A and B), continuous performance task, Stroop test, and reading span test. Details are provided elsewhere (Appendix II in the online-only Data Supplement). Neuropsychologists blinded to the clinical data performed the tests. The interval between the neuropsychological tests and MRI was <1 month.

MRI Analysis

MRI was performed on a 3.0-T imager (Achieva TX; Philips Medical Solutions, Best, The Netherlands). Three-dimensional magnetization–prepared rapid gradient-echo T1-weighted imaging and axial single-shot spin-echo echo-planar DTI were performed to evaluate subtle gray and white matter alterations. The scan parameters are detailed elsewhere (Appendix III in the online-only Data Supplement). In addition, axial fast spin-echo T2-weighted imaging and fluid-attenuated inversion recovery imaging were also performed in patients with MMD to rule out cortical and subcortical infarctions and evaluate white matter hyperintensities.

Image Processing and Evaluation

Identification of Gray Matter Alterations

Three-dimensional magnetization–prepared rapid gradient-echo images were used to compare gray matter density voxel-by-voxel between patients with MMD and controls. The steps for voxel-based morphometry of FSL (FSL-VBM, version 4.1, http://www.fmrib.ox.ac.uk/fsl) using default parameters were followed[12,13] (Appendix IV in the online-only Data Supplement). Age was considered as a covariate. A $P<0.05$ after correction for family-wise error was considered statistically significant.

Identification of White Matter Alterations

To identify subtle white matter alterations, the 4 major DTI indices (FA, MD, AD, and RD) were first extracted from the DTI using the Diffusion Toolbox of FSL and the default parameters.[12–14] Correction for eddy current distortions and motion was performed before extracting the indices. Differences in the major DTI indices between patients with MMD and controls were then tested using tract-based spatial statistics, which is a part of FSL. The default parameters and steps recommended by the software developers were used (Appendix V in the online-only Data Supplement). Age was a covariate, and results were corrected for multiple comparisons across space using threshold-free cluster enhancement. For each major DTI index, the mean value and number of voxels reaching statistical significance (threshold-free cluster enhancement-corrected; $P<0.05$) were calculated.

Probabilistic tractography was performed using FLIRT and BEDPOSTX (Appendix VI in the online-only Data Supplement). Sixteen cortical regions and bilateral thalami, which mediate intelligence, working memory, executive function/attention were selected as the seed regions. The entire brain was selected as the target region. For each probabilistic tract, the number of voxels and mean FA value were calculated.

Correlation of Microstructural Alterations With Hemodynamic Compromise and Neurocognitive Function

Voxels with abnormal gray matter density in patients with MMD were tested for correlation with the major DTI white matter indices. Any gray or white matter alterations were tested for correlation with age, presence of ischemic symptoms, hemodynamic compromise, and neuropsychological performance. Pearson product-moment correlation analysis (correlation with age, Wechsler Adult Intelligent scale-III, TMT A and B) or permutation tests performed >10 000× (presence of ischemic symptoms, hemodynamic compromise, Wisconsin Card Sorting Test, Stroop test, continuous performance task, and reading span test; a cutoff value was applied for the latter 4 tests) were used for these purposes. For all correlations or comparisons, a $P<0.05$ was considered statistically significant.

Results

Patient Characteristics

Patient characteristics are summarized in Table. There were no significant differences in age ($P=0.47$) and sex ($P=0.35$) between patients and controls. Cerebral blood flow at rest, cerebrovascular reactivity, and prevalence of comorbid risk factors did not vary significantly between the symptomatic (ie, transient ischemic attack, n=10 and asymptomatic, n=13) patients. White matter hyperintensities were observed in 10 (43.5%) patients with MMD on T2-weighted or fluid-attenuated inversion recovery images. Hyperintensities were also more frequent in the symptomatic patients (7/10; $P<0.05$). The mean full-scale intelligence quotient of patients with MMD was 94±13. The neuropsychological assessment results of the patients are summarized in Table I in the online-only Data Supplement. There were no significant differences in the full-scale intelligence quotient or scores of other Wechsler Adult Intelligent scale indices or other components of the neuropsychological battery between symptomatic and asymptomatic patients.

Gray Matter Alterations

FSL-VBM revealed a significant reduction in the density of the bilateral posterior cingulate cortex (PCC; Figure 1).

Table. Patient Characteristics

Sex	Age, y	Clinical Presentation	Location of WMH	Suzuki Grade		Hemodynamic Compromise		Comorbid Illness
				Right	Left	Right	Left	
F	58	Asymptomatic	Right deep white matter	3	4	None	None	
F	36	TIA	Bilateral deep white matter	3	3	None	None	
F	49	TIA	Bilateral frontal deep white matter	3	3	None	None	
F	33	TIA	None	3	4	None	None	Hypertension
F	51	Asymptomatic	None	3	4	None	None	
M	49	Asymptomatic	None	3	3	None	None	
M	42	Asymptomatic	None	1	4	None	None	
F	53	Asymptomatic	None	4	2	None	None	
F	34	Asymptomatic	None	3	3	None	None	
F	40	TIA	Right frontal white matter	3	2	Moderate	Moderate	Hypertension
F	40	TIA	Right frontal white matter	2	2	None	None	
F	25	TIA	Bilateral deep white matter	3	3	Moderate	Moderate	Hyperlipidemia
F	46	Asymptomatic	None	4	4	None	None	
F	47	TIA	Bilateral deep white matter	4	4	None	None	
M	43	Asymptomatic	None	3	3	Moderate	Moderate	
F	21	Asymptomatic	Right parietal deep white matter	3	1	None	None	
F	49	Asymptomatic	None	3	5	Severe	Severe	Diabetes mellitus
F	36	Asymptomatic	None	3	2	Moderate	None	
M	44	TIA	None	3	3	Severe	Severe	
F	39	Asymptomatic	None	3	2	Severe	Moderate	
F	46	TIA	Bilateral deep white matter	3	3	Moderate	None	Hypertension
M	23	TIA	None	3	3	Severe	Moderate	
M	36	Asymptomatic	Left frontal deep white matter	3	3	Moderate	Moderate	

Asymptomatic: Patients with neurological episodes such as syncope and transient ischemic attack (TIA) in childhood but remained asymptomatic after adolescence. Hemodynamic compromise was rated as severe when cerebrovascular reactivity (CVR) was <5% from the baseline, moderate when 5≤CVR<10%, and normal when 10%≤CVR. 10% (Appendix I in the online-only Data Supplement). WMH indicates white matter hyperintensities.

White Matter Alterations

Tract-based spatial statistics showed a significant widespread FA decrease and RD increase in patients with MMD, (55.2% and 42.5%, respectively, of the entire skeleton; Figure 2). Some voxels with FA and RD alterations also revealed significant MD increases. Voxels showing MD increases occupied 20.9% of the mean FA skeleton. Regarding AD, no voxels survived after correction for multiple comparisons, although AD decreases were observed mainly at the superior longitudinal fasciculus and cingulate bundle when correction was not performed (uncorrected $P<0.05$).

Probabilistic tractography also revealed decreases in the mean FA of several white matter tracts in patients with MMD. The number of voxels of each tract of patients with MMD did not vary significantly from that of controls.

Correlation of Microstructural Alterations With Hemodynamic Compromise and Neurocognitive Function

The density of the cingulate cortex of the patients significantly correlated with the mean FA ($r=0.54$; $P<0.0001$) or RD ($r=-0.41$; $P<0.01$) of the white matter skeleton (Figure 3).

The density of the bilateral PCC (http://fmri.wfubmc.edu/software/PickAtlas) and the mean FA of the white matter skeleton of patients with MMD had inverse associations with age ($r=-0.43$; $P<0.01$ and $r=-0.57$; $P<0.005$, respectively; Figure I in the online-only Data Supplement). The local gray matter density or major DTI indices did not vary significantly between symptomatic and asymptomatic patients. Patients with hemodynamic compromise had significantly lower PCC densities than their counterparts, but the means of each major DTI index of the white matter skeleton did not vary between these 2 groups.

Both the PCC density and mean values of the major DTI indices of the white matter skeleton were not significantly associated with neuropsychological performance. However, the mean FA of the following white matter tracts significantly associated with neuropsychological performance (Table II in the online-only Data Supplement; Figure 4); the fibers originating from the left superior frontal with the processing speed ($r=0.45$); left middle frontal, left supramarginal gyrus, and right supramarginal gyrus with TMT A ($r=0.43$, 0.43, and 0.48, respectively); and left PCC with TMT B and A ($r=0.43$). The mean FA values of the tracts originating from the right

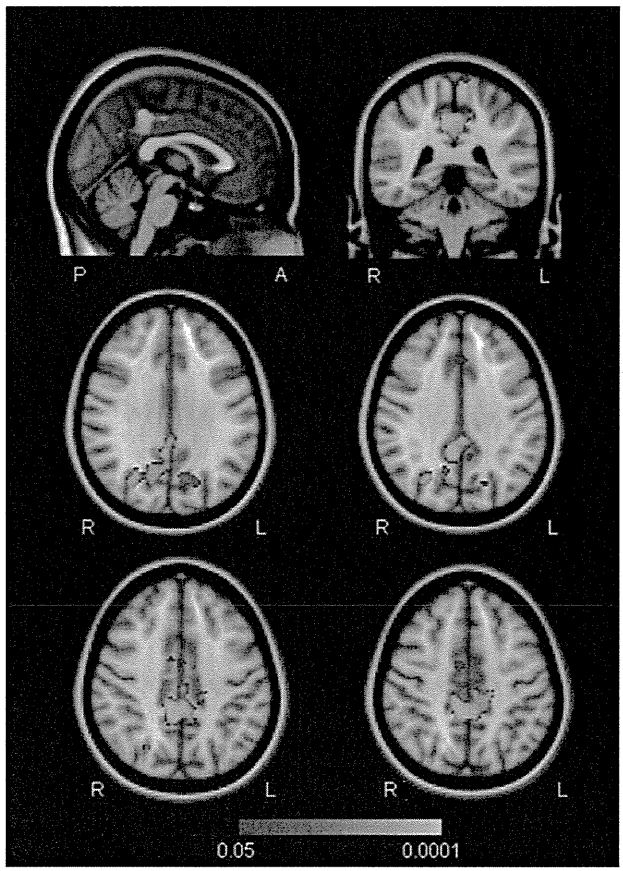

Figure 1. Comparison of the gray matter density between the patients moyamoya disease (MMD) and controls. Decreased gray matter density is observed in the bilateral posterior cingulate cortex of patients with MMD and is highlighted in shades of blue (family-wise error-corrected: $P<0.05$). The color scale represents the P values.

superior frontal, right middle frontal, and left middle cingulate cortex of patients with higher Stroop test performance were significantly higher than those of their counterparts. Similarly, these values of the tracts originating from the bilateral middle frontal, right anterior cingulate cortex, and left middle cingulate cortex were significantly higher in patients with higher reading span test performance than their counterparts.

Discussion

Adult patients with MMD suffer long disease duration. Thus, adult MMD is useful for studying the subtle effects of chronic hypoperfusion on the brain microstructure. This study revealed a decrease in the bilateral PCC density and widespread white matter areas with an FA decrease and RD increase in patients with MMD, alterations that were associated with age. In addition, the bilateral PCC density was significantly associated with hemodynamic compromise, and the mean FA values of the white matter tracts of the dorsolateral prefrontal, cingulate, and inferior parietal regions were significantly associated with neuropsychological performance.

PCC is associated with arousal, attention, internally directed thoughts, and environmental change detection.[15] Focal lesion confined to PCC has rarely been reported, therefore, neurocognitive consequences have remained unclear. In stroke, memory disturbances rather than a perceptual error has been reported, however, concomitant involvement in the fornix and the corpus callosum might have been responsible for the cognitive dysfunctions in a large part.[16] Connectivity of PCC is reduced in aging, trauma, Alzheimer disease, autism, schizophrenia, depression, and attention deficit hyperactivity disorder.[15,17,18] PCC comprises part of the default mode network and its failure to deactivate during the task is considered responsible for the attention lapses.[19] In this study, we speculate that the volume reduction in the cingulate may be because of the reduced white matter connectivity. Vulnerability of the posterior part of the cingulum may be explained by its high energetic demand, where PCC consumes 40% greater cerebral blood flow and glucose compared with other brain lesions.[20]

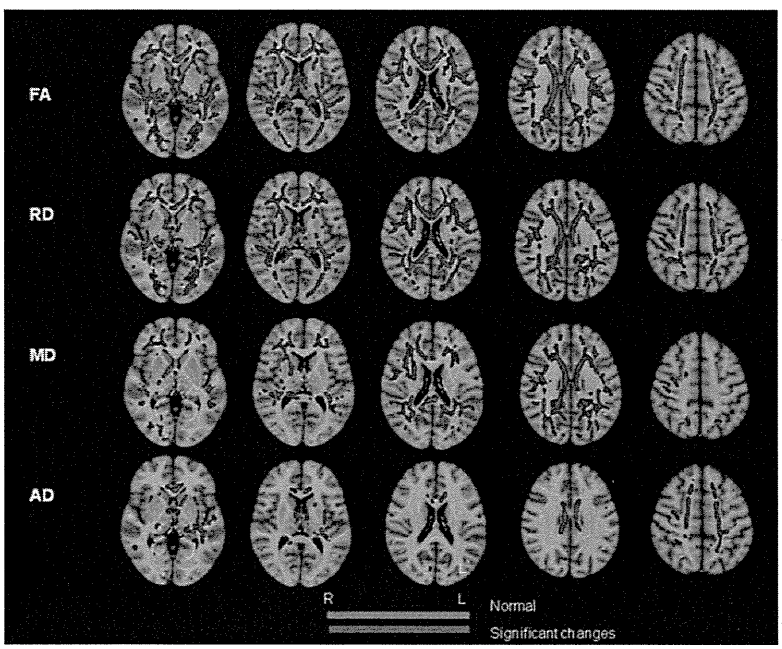

Figure 2. Results of whole brain voxel-based analysis of white matter using tract-based spatial statistics showing alterations in the 4 major diffusion tensor imaging indices. Voxels with a significant fractional anisotropy (FA) decrease, radial diffusivity (RD) increase, and mean diffusivity (MD) increase are shown (threshold-free cluster enhancement-corrected $P<0.05$). Axial diffusivity (AD) alterations are shown without corrections for multiple comparisons (uncorrected $P<0.05$).

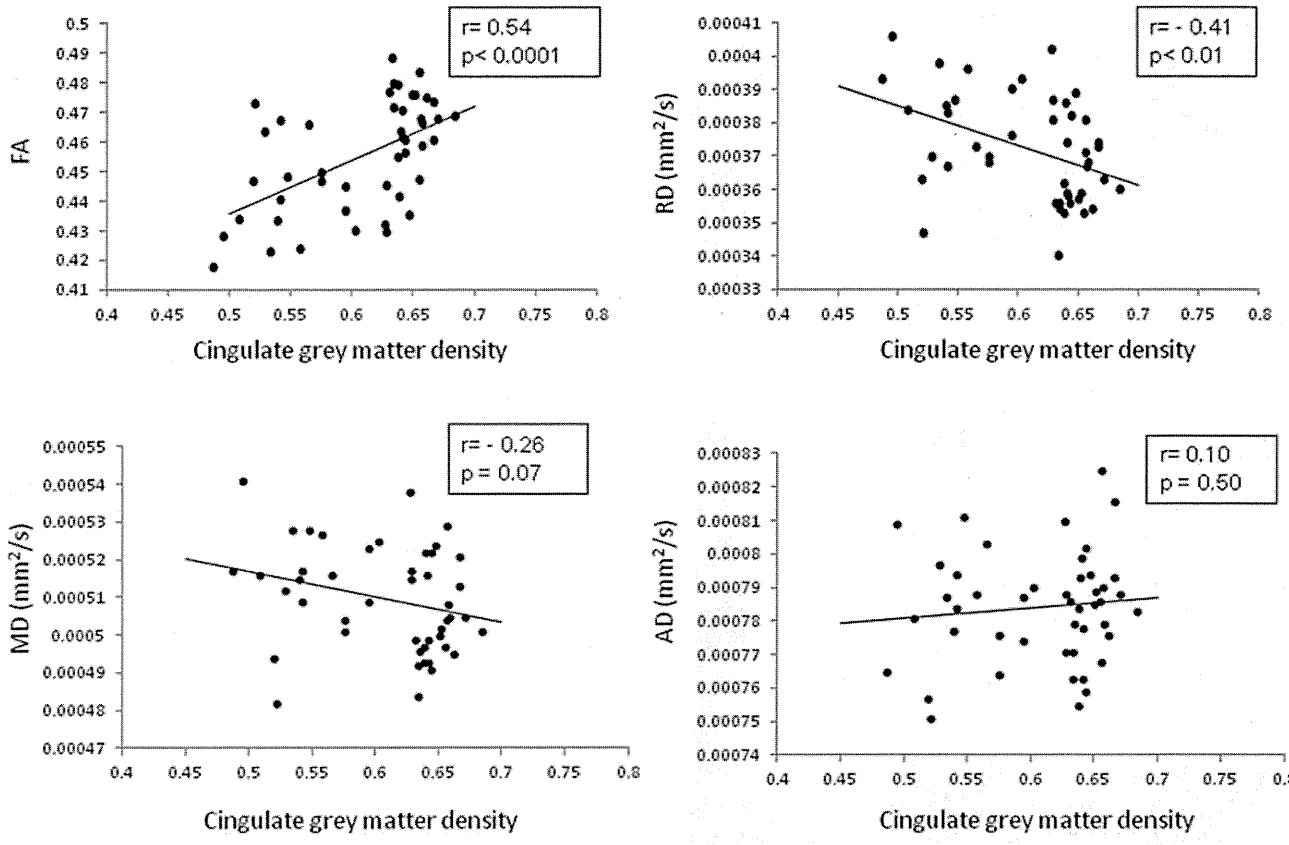

Figure 3. The scatterplots show the relationship between the mean values of each major diffusion tensor imaging index of the entire white matter skeleton and the gray matter density of the cingulate cortex. Significant positive and inverse correlations were observed between the mean fractional anisotropy (FA; r=0.54; P<0.0001) and radial diffusivity (RD; r=–0.41; P<0.01) and the gray matter density, respectively. AD indicates axial diffusivity; and MD, mean diffusivity.

We speculate that PCC is one of the key neural substrates of attention deficit frequently observed in adult MMD.

White matter is vulnerable to chronic ischemia.[21] The reported white matter changes in chronic ischemia include demyelination, axonal loss, and gliosis.[22–24] The observed altered DTI indices of white matter also reflect these changes. The major DTI indices are sensitive to changes in the brain's microstructure associated with myelination, axonal membrane integrity, axon and glial density, and coherence of axonal orientation.[25] Generally, neuronal or axonal loss and myelin degeneration are associated with MD increase, which is because of the loss of cell structures that restrict water molecular diffusion, and with FA decrease, which is because of a decline in the alignment degree of highly organized cellular structures (axons and myelin). The observation of a wider area of FA alterations than MD alterations suggests that FA is more sensitive to white

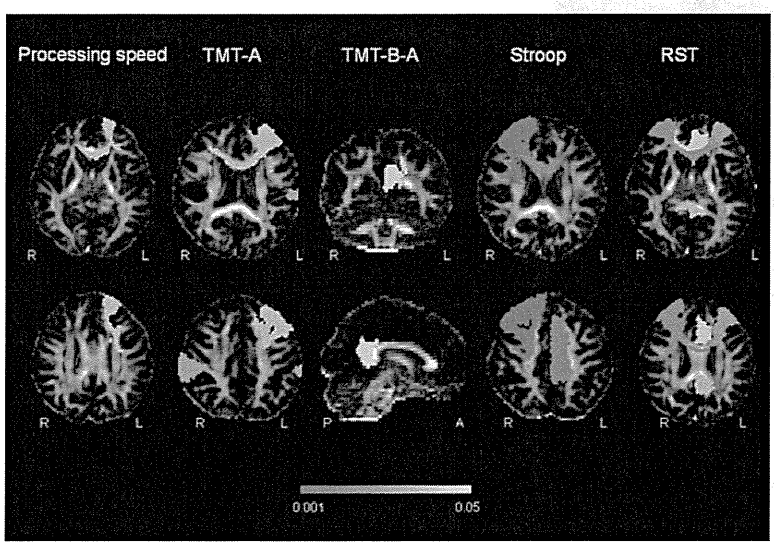

Figure 4. The spatial distribution of areas revealing significant correlations between the mean fractional anisotropy (FA) of white matter tracts derived by probabilistic tractography and neuropsychological performance (uncorrected P<0.05). Results of probabilistic tractography of a patient are shown. Processing speed significantly correlated with the mean FA of the tracts originating from the left superior frontal (SF) gyrus; Trail Making Test (TMT) A with the left middle frontal (MF) and bilateral supramarginal gyrus; TMT B and A with the left posterior cingulate cortex; the Stroop test with the right SF, MF, and the left middle cingulate cortex (MCC); and the reading span test (RST) with the right SF, bilateral MF, right anterior cingulate cortex, and left MCC. The color scale represents the P values.

matter alterations. More specific information about myelin and axonal damage can be obtained by incorporating the directional DTI metrics, such as RD and AD. The former reportedly reflects the degree of myelin breakdown, whereas the latter reflects axonal damage and Wallerian degeneration.[26,27] The preferential increase in RD observed in this study may reflect that the major pathological change in white matter in MMD is from demyelination/myelin breakdown. In this study, the exploratory analysis revealed a trend toward AD decrease in the long white matter tracts that run posteroanteriorly, although none of these voxels survived after correction for multiple comparisons. The tendency toward AD decreases in these tracts may reflect axonal swelling associated with Wallerian degeneration. We hypothesize that these white matter tracts are more vulnerable to ischemia compared other tracts.

In this study, the altered white matter integrity did not significantly associate with hemodynamic compromise. Taken together, the observed correlations between the mean FA of the white matter skeleton and age suggest that the disease duration may have a higher effect on white matter integrity than the severity of ischemia.[7,8] Alternatively, chronic ischemia in MMD may lower the threshold for age-related decline in white matter integrity.[21] Our results also showed an age-related decline in the PCC density, which suggests regional variation in vulnerability to chronic ischemia. The present results may provide some insight into the potential role of the revascularization surgery. It is conceivable that the already damaged gray and white matter may be less likely to normalize even after hemodynamic improvements. Given that the duration of chronic ischemia rather than severity may have more effect on the white matter integrity, early surgical intervention might be effective for preventing microstructural damage and cognitive dysfunctions in adults. Similarly, early surgical intervention may facilitate normal white matter development and intellectual outcome in children.

Consistent with previous reports, impaired executive function/attention and working memory were observed in ≈30% of patients with MMD.[2,3,28] In this study, we investigated the role of the dorsolateral prefrontal cortex, inferior parietal lobe, and cingulate cortex because these areas are reportedly associated consistently with executive function and working memory/attention.[29–31] The mean FA values of the dorsolateral prefrontal area (middle and superior frontal gyri) significantly correlated with neuropsychological performance, suggesting that the area serves as a domain for working memory, executive function, and attention. This observation is consistent with that of previous studies demonstrating the association between cognitive function and the integrity of white matter fiber tracts integrating the frontoparietal cortical areas.[29] The frontoparietal control network constitutes the dorsolateral prefrontal cortex, anterior cingulate cortex, presupplementary motor area, anterior insula, and PCC.[15] It should be emphasized that the mean FA values of the fibers originating from the left PCC were associated with TMT B and A in this study. TMT B and A is not associated with visuoperceptual and working memory and serves as a relatively pure indicator of executive control abilities.[32] This observation indicates that the white matter connection from PCC is associated with executive function.

This study had some limitations. First, the study population was small. The lack of neuropsychological data for assessing the frontal lobe functions in the controls may have resulted in a lack of statistical significance across comparisons. Second, the seed regions putatively associated with frontal lobe-mediated cognitive functions were used for probabilistic tractography. However, previous functional MRI studies demonstrated that the temporal lobe is also associated with working memory.[33] Third, white matter integrity is associated with age and sex.[34] Sex was not completely matched in the study population and may have influenced the results of the comparison between patients and controls. Further investigation in a large population, preferably a multicenter study, is warranted to help identify the prevalence of cognitive dysfunction and the relationship with other neuroimaging markers,[35] which will ultimately lead to determine optimal indication for the revascularization surgery.

Conclusions

Steno-occlusive changes in the major cerebral arteries in MMD cause microstructural brain damage, primarily in the cerebral white matter and impair executive function, working memory, and attention. The clinical significance of this study findings is that early detection of microstructural changes can enable early therapeutic intervention to improve patient cognitive outcome.

Sources of Funding

This study was supported by a grant from the Research Committee on moyamoya disease, sponsored by the Ministry of Health, Labor, and Welfare of Japan.

Disclosures

None.

References

1. Kuroda S, Houkin K. Moyamoya disease: current concepts and future perspectives. *Lancet Neurol.* 2008;7:1056–1066. doi: 10.1016/S1474-4422(08)70240-0.
2. Mogensen MA, Karzmark P, Zeifert PD, Rosenberg J, Marks M, Steinberg GK, et al. Neuroradiologic correlates of cognitive impairment in adult Moyamoya disease. *AJNR Am J Neuroradiol.* 2012;33:721–725. doi: 10.3174/ajnr.A2852.
3. Karzmark P, Zeifert PD, Bell-Stephens TE, Steinberg GK, Dorfman LJ. Neurocognitive impairment in adults with moyamoya disease without stroke. *Neurosurgery.* 2012;70:634–638. doi: 10.1227/NEU.0b013e3182320d1a.
4. Whitwell JL, Jack CR Jr. Comparisons between Alzheimer disease, frontotemporal lobar degeneration, and normal aging with brain mapping. *Top Magn Reson Imaging.* 2005;16:409–425. doi: 10.1097/01.rmr.0000245457.98029.e1.
5. Williams LM. Voxel-based morphometry in schizophrenia: implications for neurodevelopmental connectivity models, cognition and affect. *Expert Rev Neurother.* 2008;8:1049–1065. doi: 10.1586/14737175.8.7.1049.
6. Calviere L, Ssi Yan Kai G, Catalaa I, Marlats F, Bonneville F, Larrue V. Executive dysfunction in adults with moyamoya disease is associated with increased diffusion in frontal white matter. *J Neurol Neurosurg Psychiatry.* 2012;83:591–593. doi: 10.1136/jnnp-2011-301388.
7. Jeong H, Kim J, Choi HS, Kim ES, Kim DS, Shim KW, et al. Changes in integrity of normal-appearing white matter in patients with moyamoya disease: a diffusion tensor imaging study. *AJNR Am J Neuroradiol.* 2011;32:1893–1898. doi: 10.3174/ajnr.A2683.
8. Conklin J, Fierstra J, Crawley AP, Han JS, Poublanc J, Mandell DM, et al. Impaired cerebrovascular reactivity with steal

phenomenon is associated with increased diffusion in white matter of patients with Moyamoya disease. *Stroke*. 2010;41:1610–1616. doi: 10.1161/STROKEAHA.110.579540.
9. Jurcoane A, Keil F, Szelenyi A, Pfeilschifter W, Singer OC, Hattingen E. Directional diffusion of corticospinal tract supports therapy decisions in idiopathic normal-pressure hydrocephalus. *Neuroradiology*. 2014;56:5–13. doi: 10.1007/s00234-013-1289-8.
10. Research Committee on the Pathology and Treatment of Spontaneous Occlusion of the Circle of Willis. Guidelines for diagnosis and treatment of moyamoya disease (spontaneous occlusion of the circle of willis). *Neurolo Med Chir*. 2012;52:245–266.
11. Matsuoka K, Uno M, Kasai K, Koyama K, Kim Y. Estimation of premorbid IQ in individuals with Alzheimer's disease using Japanese ideographic script (Kanji) compound words: Japanese version of National Adult Reading Test. *Psychiatry Clin Neurosci*. 2006;60:332–339. doi: 10.1111/j.1440-1819.2006.01510.x.
12. Behrens TE, Woolrich MW, Jenkinson M, Johansen-Berg H, Nunes RG, Clare S, et al. Characterization and propagation of uncertainty in diffusion-weighted MR imaging. *Magn Reson Med*. 2003;50:1077–1088. doi: 10.1002/mrm.10609.
13. Woolrich MW, Jbabdi S, Patenaude B, Chappell M, Makni S, Behrens T, et al. Bayesian analysis of neuroimaging data in FSL. *Neuroimage*. 2009;45:S173–S186.
14. Smith SM, Jenkinson M, Woolrich MW, Beckmann CF, Behrens TE, Johansen-Berg H, et al. Advances in functional and structural MR image analysis and implementation as FSL. *Neuroimage*. 2004;23(suppl 1):S208–S219. doi: 10.1016/j.neuroimage.2004.07.051.
15. Leech R, Sharp DJ. The role of the posterior cingulate cortex in cognition and disease. *Brain*. 2014;137:12–32.
16. Valenstein E, Bowers D, Verfaellie M, Heilman KM, Day A, Watson RT. Retrosplenial amnesia. *Brain*. 1987;110 (pt 6):1631–1646.
17. Baron JC, Chételat G, Desgranges B, Perchey G, Landeau B, de la Sayette V, et al. In vivo mapping of gray matter loss with voxel-based morphometry in mild Alzheimer's disease. *Neuroimage*. 2001;14:298–309. doi: 10.1006/nimg.2001.0848.
18. Chételat G, Desgranges B, De La Sayette V, Viader F, Eustache F, Baron JC. Mapping gray matter loss with voxel-based morphometry in mild cognitive impairment. *Neuroreport*. 2002;13:1939–1943.
19. Greicius MD, Srivastava G, Reiss AL, Menon V. Default-mode network activity distinguishes Alzheimer's disease from healthy aging: evidence from functional MRI. *Proc Natl Acad Sci U S A*. 2004;101:4637–4642. doi: 10.1073/pnas.0308627101.
20. Raichle ME, MacLeod AM, Snyder AZ, Powers WJ, Gusnard DA, Shulman GL. A default mode of brain function. *Proc Natl Acad Sci U S A*. 2001;98:676–682. doi: 10.1073/pnas.98.2.676.
21. Black S, Gao F, Bilbao J. Understanding white matter disease: Imaging-pathological correlations in vascular cognitive impairment. *Stroke*. 2009;40:S48–S52.
22. Kurumatani T, Kudo T, Ikura Y, Takeda M. White matter changes in the gerbil brain under chronic cerebral hypoperfusion. *Stroke*. 1998;29:1058–1062.
23. Shibata M, Ohtani R, Ihara M, Tomimoto H. White matter lesions and glial activation in a novel mouse model of chronic cerebral hypoperfusion. *Stroke*. 2004;35:2598–2603. doi: 10.1161/01.STR.0000143725.19053.60.
24. Riddle A, Dean J, Buser JR, Gong X, Maire J, Chen K, et al. Histopathological correlates of magnetic resonance imaging-defined chronic perinatal white matter injury. *Ann Neurol*. 2011;70:493–507. doi: 10.1002/ana.22501.
25. Beaulieu C. The basis of anisotropic water diffusion in the nervous system - a technical review. *NMR Biomed*. 2002;15:435–455. doi: 10.1002/nbm.782.
26. Harsan LA, Poulet P, Guignard B, Steibel J, Parizel N, de Sousa PL, et al. Brain dysmyelination and recovery assessment by noninvasive in vivo diffusion tensor magnetic resonance imaging. *J Neurosci Res*. 2006;83:392–402. doi: 10.1002/jnr.20742.
27. Song SK, Yoshino J, Le TQ, Lin SJ, Sun SW, Cross AH, et al. Demyelination increases radial diffusivity in corpus callosum of mouse brain. *Neuroimage*. 2005;26:132–140. doi: 10.1016/j.neuroimage.2005.01.028.
28. Calviere L, Catalaa I, Marlats F, Viguier A, Bonneville F, Cognard C, et al. Correlation between cognitive impairment and cerebral hemodynamic disturbances on perfusion magnetic resonance imaging in European adults with moyamoya disease. Clinical article. *J Neurosurg*. 2010;113:753–759. doi: 10.3171/2010.4.JNS091808.
29. Barbey AK, Koenigs M, Grafman J. Dorsolateral prefrontal contributions to human working memory. *Cortex*. 2013;49:1195–1205. doi: 10.1016/j.cortex.2012.05.022.
30. Cheng HL, Lin CJ, Soong BW, Wang PN, Chang FC, Wu YT, et al. Impairments in cognitive function and brain connectivity in severe asymptomatic carotid stenosis. *Stroke*. 2012;43:2567–2573. doi: 10.1161/STROKEAHA.111.645614.
31. Weissman DH, Giesbrecht B, Song AW, Mangun GR, Woldorff MG. Conflict monitoring in the human anterior cingulate cortex during selective attention to global and local object features. *Neuroimage*. 2003;19:1361–1368.
32. Sánchez-Cubillo I, Periáñez JA, Adrover-Roig D, Rodríguez-Sánchez JM, Ríos-Lago M, Tirapu J, et al. Construct validity of the trail making test: role of task-switching, working memory, inhibition/interference control, and visuomotor abilities. *J Int Neuropsychol Soc*. 2009;15:438–450. doi: 10.1017/S1355617709090626.
33. Park DC, Welsh RC, Marshuetz C, Gutchess AH, Mikels J, Polk TA, et al. Working memory for complex scenes: age differences in frontal and hippocampal activations. *J Cogn Neurosci*. 2003;15:1122–1134. doi: 10.1162/089892903322598094.
34. Inano S, Takao H, Hayashi N, Abe O, Ohtomo K. Effects of age and gender on white matter integrity. *AJNR Am J Neuroradiol*. 2011;32:2103–2109. doi: 10.3174/ajnr.A2785.
35. Zaharchuk G, Do HM, Marks MP, Rosenberg J, Moseley ME, Steinberg GK. Arterial spin-labeling MRI can identify the presence and intensity of collateral perfusion in patients with moyamoya disease. *Stroke*. 2011;42:2485–2491. doi: 10.1161/STROKEAHA.111.616466.

ONLINE SUPPLEMENT

Appendix-I: Hemodynamic status assessment

Cerebrovascular reactivity (CVR) was expressed as the percent changes of the regional cerebral blood flow (rCBF) from the baseline after intravenous acetazolamide injection. CVR less than 15 % in the left or right middle cerebral artery territory was considered as hemodynamic compromise. In 5 of 13 asymptomatic MMD patients, the hemodynamic status had already been evaluated by using positron emission computed tomography (PET) in 2004-2009. All of them had normal resting state rCBF, cerebral blood volume and oxygen extraction fraction. As none of them had ischemic episode, no further hemodynamic assessment was carried out. These patients were rated as free of hemodynamic compromise based on the results of PET study.

Appendix-II: Neuropsychological assessment

The WAIS-III provides the index scores for overall intellectual ability (Full-scale IQ), language, verbal ability (Perception Reasoning/ Organization Index), auditory attention and mental manipulation (Working Memory/ Freedom from Distractibility Index), and visual-motor speed (Processing Speed Index) — with the mean score of 100 and standard deviation of 20.

The WCST measures the ability for strategic planning, organized search, utilization of environmental feedback to shift cognitive sets, directing behavior toward achieving a goal, and modulating impulsive responding[1]. It is known as a measure of executive function.

The Trail-Making Test - Part A and B assess the speed of information processing and executive functioning, respectively.

The CPT measures a person's sustained and selective attention and impulsivity. It is composed of repetitive, "boring" task that requires concentration over a period of time.

The Stroop test measures sustained attention. A reaction time delay was examined in naming the color of the word printed in an unmatched color.

The RST is a complex verbal test which evaluates both storage and processing (i.e., reading) elements of working memory[2]. The scores are expressed as the total number and proportion of words correctly recalled.

Appendix-III: The MR imaging scan parameters

The scan parameters for DTI were as follows: repetition time (TR)/echo time (TE)/flip angle = 5051 ms/85 ms/90°, field of view = 224 x 224 mm^2, matrix size = 128 × 128, b-value = 1000 s mm^{-2}, the number of diffusion gradient directions = 32, slice thickness = 3 mm, the number of slices = 43, and the number of excitation =1. The 3D-MPRAGE was performed with TR/TE/flip angle = 6.8 ms/3.1ms/ 8° and inversion time (TI) = 1100 ms. The scan parameters for T2-weighted imaging were TR/TE = 4137 ms/90 ms and effective echo train length = 15. Those for FLAIR imaging were TR/TE = 10000 ms/100 ms and TI = 2700 ms.

Appendix-IV: Comparison of grey matter density

The 3D-MPRAGE images were brain-extracted and grey matter-segmented before being registered to the MNI 152 standard space using non-linear registration. The resulting images were then averaged and flipped along the x-axis to create a left-right symmetric, study-specific grey matter template. Next, all native grey matter images were non-linearly registered to this study-specific template and modulated to correct for local expansion due to the non-linear component of the spatial transformation. The modulated grey matter images were then smoothed with an isotropic Gaussian kernel with sigma of 3mm. Finally, voxelwise general linear model was applied using a permutation-based non-parametric testing.

Appendix-V: TBSS

TBSS was used to align all subjects' FA images to FMRIB58_FA standard-space image and affine the aligned images into 1x1x1 mm^3 MNI152 standard space. An average FA image was created for each section. Then, the average FA images were used to create a mean FA skeleton by applying a threshold of 0.2. Cross-subject statistics were performed for the voxels that form the skeleton. The nonlinear warps and skeleton projection were then applied to the other DTI indices, i.e., radial diffusivity (RD), mean diffusivity (MD), and axial diffusivity (AD). TBSS of RD, MD, and AD was subsequently performed.

Appendix-VI: Probabilistic tractography

The seed regions were generated by using automated anatomical atlas (AAL), and were transformed into the native T1-weighted images using FLIRT algorithm. For fiber tracking, the probability distribution of diffusion directions in each voxel was estimated by using Bayesian sampling techniques

(BEDPOSTX). The voxels which had fewer streamlines than 15% of the maximum number of streamlines across all voxels in each reconstructed tract were excluded. The reconstructed probability maps in each region were transformed to the binary images. Seed mask images were subtracted from the binarized probability maps for creating white matter masks to measure the mean FA values of subcortical tissue.

Supplemental Table I. The neuropsychological performance of the MMD patients

Study		cut-off	The range (mean ± SD) of scores achieved by all patients	Percent of patients with the scores lower than the cut-off value	The mean (SD) score achieved by the asymptomatic patients	The mean (SD) score achieved by the symptomatic patients	p
WAIS -III							
	verbal IQ	80	64-121 (95±13)	4.3%	98.9 (12.4)	92.1 (13.0)	0.2279
	motor IQ	80	71-113 (93±11)	17.4%	95.6 (11.1)	90.3 (11.7)	0.2937
	full scale IQ	80	65-120 (94±13)	8.7%	97.1 (12.4)	91.4 (12.9)	0.3145
subscore							
	verbal perception		61-111 (96±13)	26.1%	100.1 (10.0)	91.0 (15.0)	0.1112
	perceptual		55-114 (95±13)	17.4%	99.6 (14.7)	89.2 (14.4)	0.1278

	working memory		58-123 (93±14)	34.8%	95.3 (12.1)	89.7 (14.2)	0.3507
	processing speed		63-133 (96±15)	30.4%	95.7 (10.7)	96.2 (18.2)	0.9389
TMT-A		87	35-113 (72.2 ± 20.1)	13.0%	73.3 (18.7)	71.0 (22.6)	0.8048
TMT-B		100	58-217 (93.5± 34.8)	26.0%	85.9 (16.2)	102.5 (48.3)	0.3131
B-A		60	-25-134 (21.2±33.2)	8.7%	12.7 (15.6)	31.5 (45.5)	0.212
WSCT	CA	4	1-6 (4.9 ± 1.4)	30.4%	4.8 (1.5)	5.0 (1.2)	0.212
	PEM	2	0-6 (1.7 ± 1.8)	34.7%	1.7 (1.5)	1.6 (2.4)	0.764
	PEN	3	0-15 (2.6 ± 3.7)	39.1%	2.6 (2.3)	4.0 (6.3)	1
Stroop		10	2-129 (14.3 ± 26.7)	34.8%	7.8 (3.8)	22.9 (40.3)	0.11
CPT	error	3	0-71 (6 ± 14.8)	39.1%	2.5 (1.4)	10.9 (23.9)	0.1448

	RT	480 ms	312.7 - 1533 (494 ± 250.6)	34.8%	428.7 (95.2)	466.5 (100.8)	0.3878
RST		2	1.5-4 (2.5 ± 0.6)	39.1%	2.3 (0.4)	2.8 (0.8)	0.0876

Supplemental Table II. The p-values (correlation coefficient) achieved in testing the correlation/ association between the mean FA values of each cortical and subcortical-seed based probabilistic tract and Neuropsychological performance

	verbal IQ	motor IQ	f IQ	VC	PO	WM	PS	TMT -A	TMT -B	B-A	WSCT	Stroop	CPT	RST
Frontal														
Lt. SF	0.08 (0.39)	***0.06*** ***(0.40)***	0.11 (0.36)	0.10 (0.37)	0.13 (0.34)	0.28 (0.25)	**0.04** **(0.45)**	0.37 (0.20)	0.19 (0.29)	0.42 (0.18)	***0.05***	0.097	0.15	0.07
Rt. SF	0.93 (0.01)	0.92 (0.00)	0.81 (0.06)	0.82 (0.05)	0.50 (0.15)	0.48 (0.16)	0.10 (0.37)	0.79 (0.06)	0.83 (0.05)	0.70 (0.09)	0.66	**0.002**	0.89	0.18
Lt. MF	0.34 (0.22)	0.68 (0.07)	0.50 (0.14)	0.13 (0.34)	0.38 (0.20)	0.89 (0.03)	0.37 (0.21)	**0.04** **(0.43)**	0.10 (0.36)	0.60 (0.12)	0.66	0.210	0.65	**0.03**
Rt. MF	0.34 (0.20)	0.43 (0.11)	0.48 (0.13)	0.22 (0.28)	0.25 (0.26)	0.72 (0.08)	0.13 (0.34)	0.36 (0.21)	0.41 (0.18)	0.77 (0.07)	0.33	**0.004**	0.81	**0.02**
Cingulum														
Lt. ACC	0.09 (0.38)	0.14 (0.31)	***0.06*** ***(0.40)***	0.33 (0.22)	0.42 (0.18)	***0.05*** ***(0.44)***	0.16 (0.32)	0.28 (0.24)	0.89 (0.03)	0.42 (0.18)	0.55	0.139	0.88	0.08
Rt. ACC	0.39 (0.15)	0.52 (0.17)	0.45 (0.15)	0.28 (0.25)	0.13 (0.34)	0.21 (0.29)	0.64 (0.11)	0.12 (0.34)	0.35 (0.21)	0.96 (0.01)	0.44	0.744	0.84	**0.048**
Lt. DCC	0.97 (0.01)	0.89 (0.04)	0.94 (0.02)	0.69 (0.10)	0.38 (0.20)	0.81 (0.05)	0.87 (0.04)	0.26 (0.25)	0.93 (0.02)	0.57 (0.13)	0.67	**0.016**	0.90	**0.04**
Rt. DCC	0.93 (0.02)	0.88 (0.04)	0.97 (0.01)	0.99 (0.00)	0.21 (0.29)	0.72 (0.08)	0.69 (0.09)	0.37 (0.20)	0.70 (0.09)	0.34 (0.21)	0.59	0.491	0.91	0.22

Lt. PCC	0.52 (0.15)	0.27 (0.24)	0.43 (0.18)	0.65 (0.10)	0.31 (0.23)	0.28 (0.25)	0.63 (0.11)	0.05 (0.43)	0.47 (0.16)	**0.048 (0.43)**	0.91	0.957	0.17	0.98
Rt. PCC.	0.77 (0.07)	0.64 (0.10)	0.70 (0.09)	0.93 (0.02)	0.98 (0.01)	0.55 (0.14)	0.95 (0.01)	0.54 (0.14)	0.60 (0.12)	0.36 (0.21)	0.60	0.427	0.08	0.74
Parietal														
Lt. SMG	0.94 (0.03)	0.83 (0.06)	1.00 (0.00)	0.62 (0.12)	0.83 (0.05)	0.74 (0.08)	0.39 (0.20)	**0.03 (0.47)**	0.73 (0.08)	0.37 (0.20)	0.60	0.668	0.19	0.13
Rt. SMG	0.49 (0.15)	0.67 (0.11)	0.65 (0.11)	0.21 (0.29)	0.51 (0.15)	0.99 (0.00)	0.56 (0.14)	**0.03 (0.48)**	0.44 (0.17)	0.64 (0.10)	0.81	0.917	0.07	***0.0678***
Lt. ANG	0.28 (0.25)	0.80 (0.06)	0.49 (0.16)	0.31 (0.23)	1.00 (0.00)	0.42 (0.18)	0.94 (0.02)	0.21 (0.28)	0.75 (0.07)	0.27 (0.24)	0.67	0.645	0.81	0.75
Rt. ANG	0.75 (0.05)	0.67 (0.11)	0.93 (0.02)	0.54 (0.14)	0.68 (0.10)	0.50 (0.16)	0.38 (0.20)	***0.05 (0.42)***	0.85 (0.04)	0.35 (0.21)	0.81	0.774	0.27	0.20
Lt. PCUN	0.43 (0.18)	0.88 (0.04)	0.52 (0.15)	0.47 (0.17)	0.57 (0.13)	0.11 (0.36)	0.83 (0.05)	0.66 (0.10)	0.88 (0.04)	0.92 (0.02)	0.88	0.322	0.08	0.87
Rt. PCUN	0.37 (0.21)	0.47 (0.16)	0.36 (0.21)	0.60 (0.12)	0.90 (0.03)	0.21 (0.29)	0.40 (0.19)	0.74 (0.08)	0.93 (0.02)	0.77 (0.07)	0.80	0.419	0.11	0.79
Thalamus														
Lt. Thal	0.95 (0.02)	0.71 (0.07)	0.72 (0.08)	0.77 (0.07)	0.46 (0.17)	0.62 (0.12)	0.62 (0.11)	0.17 (0.30)	0.34 (0.22)	***0.06 (0.41)***	0.40	0.805	0.83	0.30
Rt. Thal	0.87 (0.04)	0.82 (0.05)	0.95 (0.01)	0.58 (0.13)	0.91 (0.03)	0.86 (0.04)	0.80 (0.06)	0.91 (0.03)	0.42 (0.18)	0.36 (0.21)	0.83	0.671	0.57	0.75

Abbreviations; IQ; Intelligent quotient score, VIQ; Vebal IQ, PIQ; Performance IQ, fIQ; full scale IQ, VC; verbal comprehension, PR; Perceptual reasoning, WM; working memory, PS; Processing speed, TMT; Trail-making test, WSCT; Wisconsin card sorting test, Stroop; Stroop test, CPT; Conceptual performance task, RST; Reading span test.

Note: Uncorrected $p<0.05$ is bolded. The p-values which approach 0.05 are bolded and shown in italic.

Supplemental Figure I

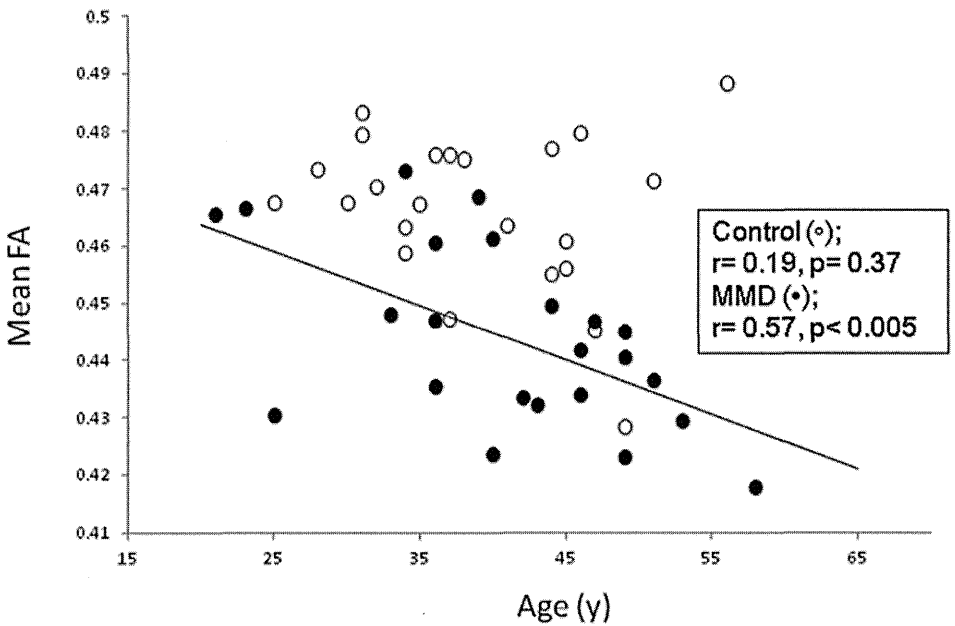

Figure legends

Appendix-Figure I.

The scatterplots show correlation between the mean FA of the white matter skeleton and age. A significant inverse correlation was observed in the MMD patients (r= -0.57, p< 0.005), but not in the control subjects (r= -0.19, p= 0.38).